Supplementary material

In vitro Splicing Assay of *ATP8B1* Gene mRNA

To verify the impact of the c.3015G>A mutation on mRNA splicing, minigene plasmids of wild-type (WT) and mutant (MT) *ATP8B1* were constructed. Using normal human genomic DNA as a template, the target fragment was PCR-amplified and cloned into the pMini - CopGFP vector (BamHI/XhoI enzyme sites), and the WT plasmid was constructed via seamless cloning (Exnase II). With the WT plasmid as a template, site-directed mutagenesis primers (ATP8B1 - MT - F/R) were designed, and the c.3015G>A mutation was introduced by PCR to construct the MT plasmid. After enzyme digestion, transformation, and sequencing verification of the recombinant plasmids, high - purity plasmids were extracted using a nontoxic plasmid midiprep kit. 293T cells were seeded in 35 mm culture dishes at a density of 50% - 60% one day before transfection. Lipofectamine 2000 was used to mediate transfection (4 μg plasmid/dish), and the medium was changed 6 hours later for continued culture. Cells were collected 48 hours after transfection. Total RNA was extracted using the TRIzol method, and cDNA was synthesized by reverse transcription. Minigene - specific primers (MiniRT - F/ATP8B1 - RT - R) were used for PCR amplification. The size differences of splicing products were analyzed by agarose gel electrophoresis, and Sanger sequencing was performed to verify whether the mutation caused abnormal splicing.

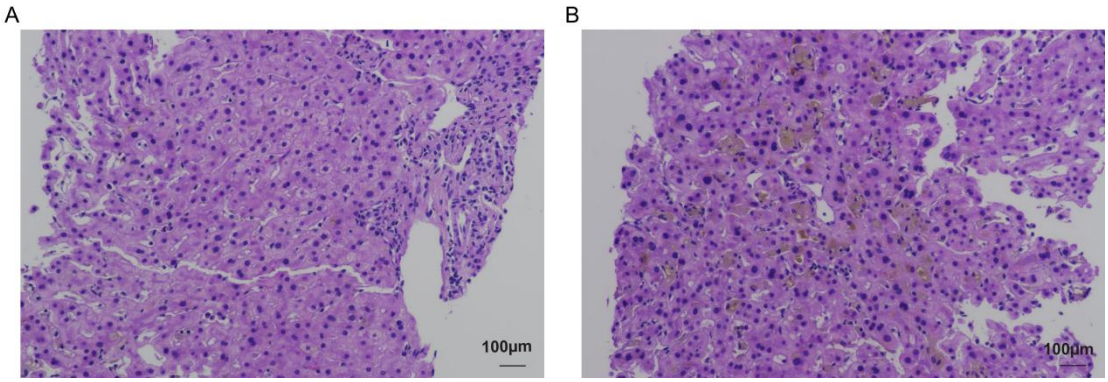

Supplementary Figure 1 Pathological findings of liver biopsy. A and B: Acute cholestatic hepatitis with moderate-severe intrahepatic cholestasis and mild (G1) inflammatory activity, in the setting of acute cholangitis (20 ×).

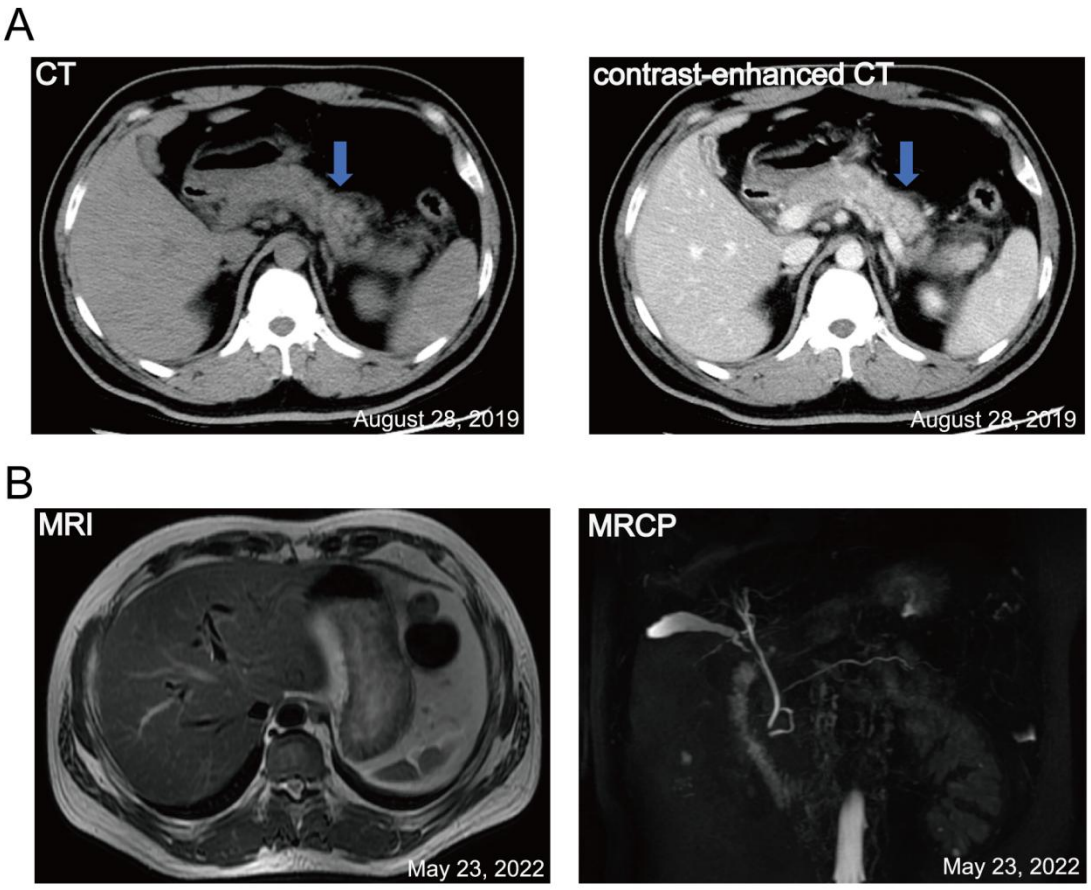

Supplementary Figure 2 Abdominal imaging findings. A: The area indicated by the blue arrow corresponds to the pancreas, which appears plump with blurred surrounding fat planes and shows strip-like areas of low density; B: MRI and MRCP examination revealed no significant focal liver lesions and no dilation of the intra- or extrahepatic bile ducts. CT: Computed tomography;

MRCP: Magnetic resonance cholangiopancreatography; MRI: Magnetic resonance imaging.

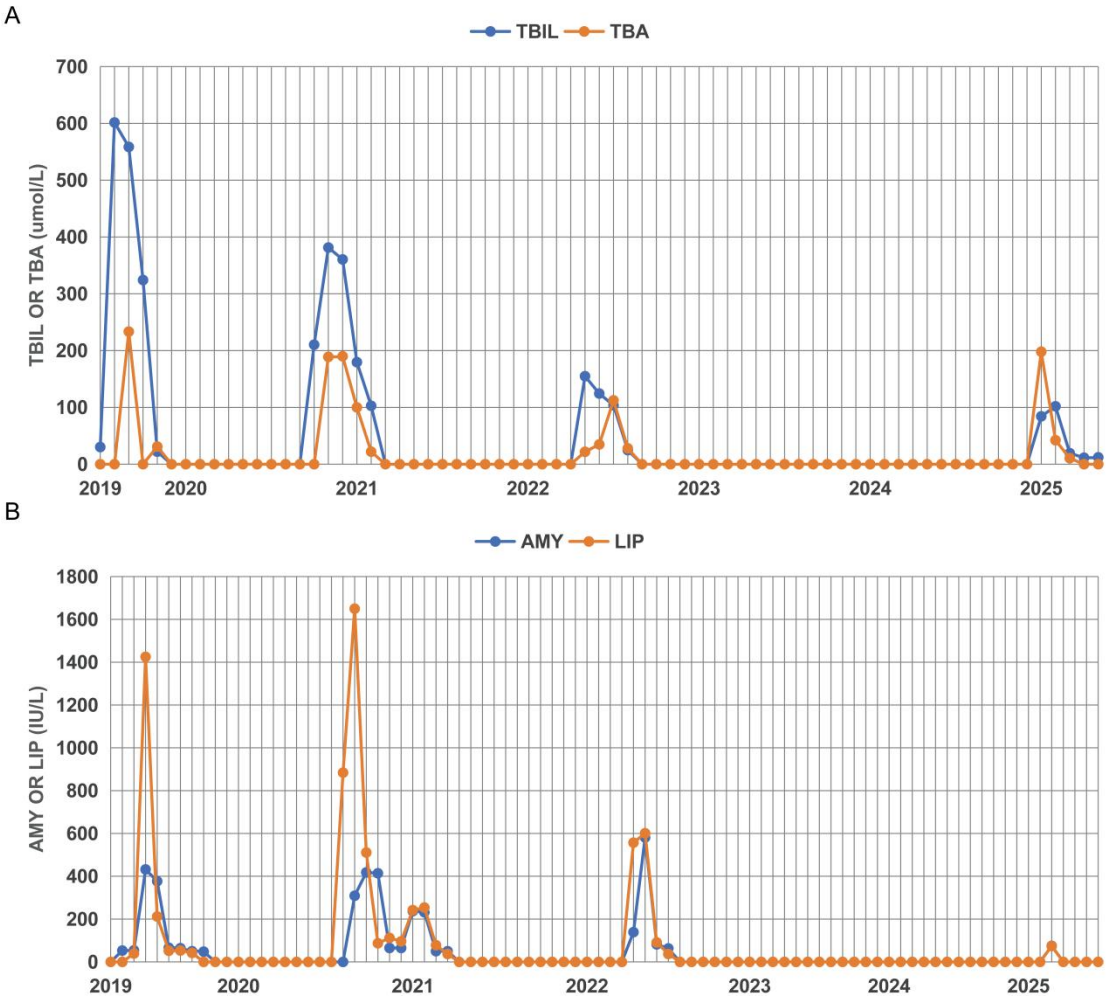

Supplementary Figure 3 The trends of total bilirubin, total bile acids, amylase, and lipase over a 6-year period. A and B: TBIL, TBA, AMY, and LIP levels have shown intermittent elevations, with normalization occurring between episodes. AMY: Amylase; LIP: Lipase; TBA: Total bile acids; TBIL: Total bilirubin.

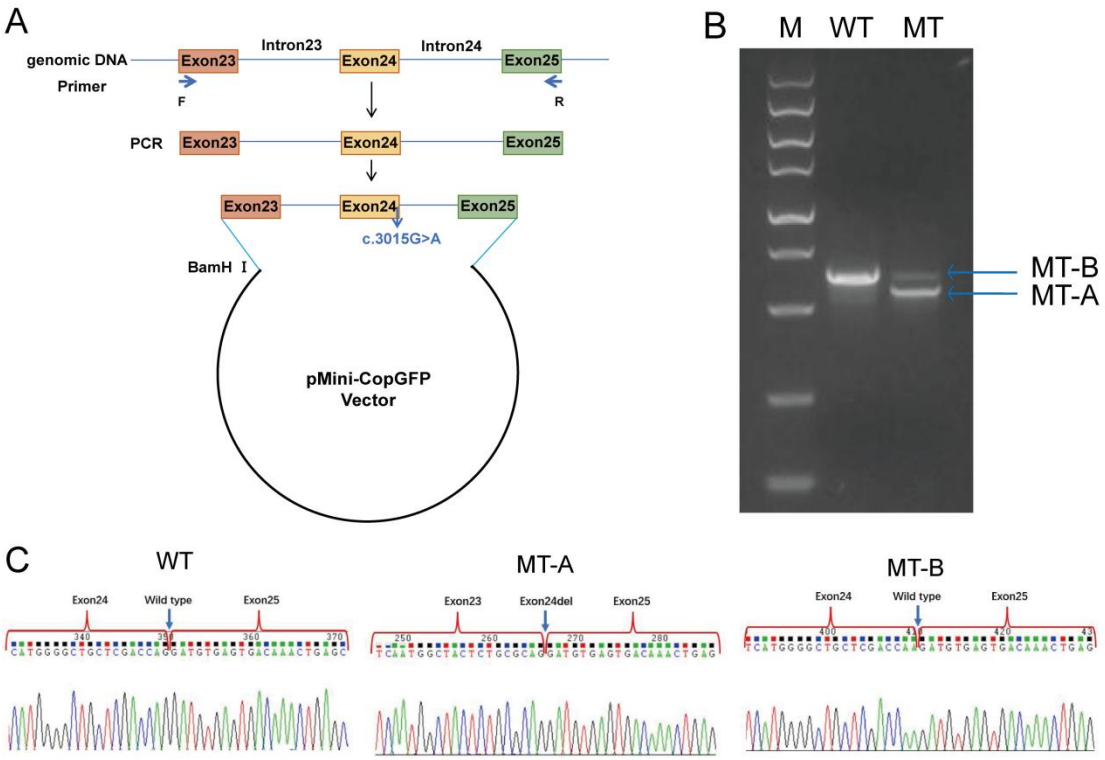

Supplementary Figure 4 Construction and validation of ATP8B1 minigene vector *via* sequencing. A: Plasmid Construction Workflow; B: Agarose gel electrophoresis of DNA fragments. Distinct banding patterns demonstrate DNA fragment variations between wild-type and mutant samples; C: Sanger sequencing analysis of exons 23–25 in WT and MT samples revealed a distinct exon 24 deletion in the MT-A variant, while the WT and MT-B samples exhibited intact exon 23–25 architecture. M: DNA molecular weight marker; MT: Mutant; WT: Wild-type.

Supplementary Table 1 Primer sequences

	Primers	Sequences
Wild - type Plasmid	ATP8B1 - F	AAGCTTGGTACCGAGCTCGGATCCCTGCCCACTATTGGCGTTGGAATAAGTGG
	ATP8B1 - R	TTAAACGGGCCCTCTAGACTCGAGCTGGAATTGACTGTTATTACAAGAGCAG
Mutant Plasmid	ATP8B1 - MT - F	TGCTCGACCAAGTAGGAGCCTCGACAAGCAG
	ATP8B1 - MT - R	TCCTACTTGGTCGAGCAGCCCATGAGGAGCA
Identification Primers	β - globin intron - F	GATATACACTGTTTGAGATGAGGA
	ATP8B1 - CX - 1R	CTCATCTGTCCAGAAGTGTC
Minigene Specific Primers	MiniRT - F	GGCTAACTAGAGAACCCCTGCTTA
	ATP8B1 - RT - R	CTGCAAATTGACTGTTATTACAAGAG